Bioactive Materials 49 (2025) 502–514

Contents lists available at ScienceDirect

Bioactive Materials

journal homepage: www.keaipublishing.com/en/journals/bioactive-materials

Exosomes from young plasma stimulate the osteogenic differentiation and prevent osteoporosis via miR-142-5p

Zhikun Li [a,b,1], Qifeng Yu [a,b,1], Xiang Cui [b,1], Yi Wang [b], Ruijun Xu [b], Renjie Lu [d], Jiahao Chen [d], Xiaohan Zhou [c], Chi Zhang [d,*], Lanya Li [c,**], Wei Xu [a,b,***]

[a] Department of Orthopedic, Shanghai General Hospital, Shanghai Jiao Tong University School of Medicine, Shanghai, 200080, China
[b] Department of Orthopedic, Tongren Hospital, School of Medicine, Shanghai Jiao Tong University, Shanghai, 200336, China
[c] The Tenth Affiliated Hospital, Southern Medical University (Dongguan People's Hospital), Dongguan, 523059, China
[d] Department of Orthopedic Surgery, Shanghai Institute of Microsurgery on Extremities, Shanghai Sixth People's Hospital Affiliated to Shanghai Jiao Tong University School of Medicine, Shanghai, 200233, China

ARTICLE INFO

Keywords:
Exosomes
Young human plasma
Old human plasma
Osteoporosis
miRNAs
Osteogenic differentiation

ABSTRACT

Osteoporosis (OP) is a multifactorial metabolic bone disorder commonly observed in the elderly, particularly prevalent in postmenopausal women. However, many conventional anti-osteoporosis drugs have undesirable side effects, limiting their long-term use. Here, we demonstrated that exosomes derived from both young and old healthy human plasma, which exhibited similar morphology, could significantly enhance the proliferation and migration of mesenchymal stem cells (MSCs). Furthermore, treatment with these exosomes increased alkaline phosphatase (ALP) activity, enhanced the mineralization of MSCs, and decreased the number of osteoclasts in vitro. When intravenously injected into rats, these exosomes accumulated in bone tissue. In vivo experiments demonstrated that both types of exosomes had a beneficial effect on osteoporosis by facilitating bone formation and suppressing osteoclast differentiation in an ovariectomized (OVX)-induced osteoporotic rat model. Strikingly, exosomes derived from young healthy human plasma exhibited stronger anti-osteoporosis effect. The miRNA sequencing analysis showed that miR-142-5p expression was significantly higher in the exosomes from young healthy adult plasma compared to in exosomes from older controls. Importantly, miR-142-5p overexpression exerted similar pro-osteogenic effects to those of exosomes from young healthy human plasma, while miR-142-5p downregulation had the opposite effect on osteogenic differentiation of MSCs. The anti-osteoporosis effect of exosomes from young healthy adult plasma were reversed upon miR-142-5p inhibition. In addition, ZFPM2 was a potential target of miR-142-5p involved in osteoporosis. Therefore, our study reveals the potential anti-osteoporosis effects of plasma exosomes and their underlying mechanisms, thereby providing an effective therapeutic strategy for clinical treatment of osteoporosis.

1. Introduction

Osteoporosis (OP) is a systemic metabolic disorder characterized by reduced bone mass and bone microstructural deterioration, resulting in fragility and an increased fracture risk [1,2]. In a rapidly aging society, OP has emerged as a significant public health concern. The imbalance between osteoclastic bone resorption and osteoblastic bone formation duringbone remodeling is a major factor leading to osteoporosis [3]. At present, there are two main treatment strategies for osteoporosis: promoting osteogenesis and inhibiting osteoclastogenesis [4]. However, drugs based on these strategies not only exhibit poor therapeutic effects but also cause some side effects (e.g. acute renal failure, osteonecrosis of the jaw, gastrointestinal intolerability and musculoskeletal pain) [5,6]. Stem cell-based therapy have recently received considerable attention in

Peer review under the responsibility of editorial board of Bioactive Materials.
* Corresponding author. Department of Orthopedic Surgery, Shanghai Institute of Microsurgery on Extremities, Shanghai Sixth People's Hospital Affiliated to Shanghai Jiao Tong University School of Medicine, Shanghai, 200233, China.
** Corresponding author. The Tenth Affiliated Hospital, Southern Medical University (Dongguan People's Hospital), Dongguan, 523059, China.
*** Corresponding author. Department of Orthopedic, Shanghai General Hospital, Shanghai Jiao Tong University School of Medicine, Shanghai, 200080, China.
E-mail addresses: hydraliskrush@sjtu.edu.cn (C. Zhang), lanyali@smu.edu.cn (L. Li), weixu@shsmu.edu.cn (W. Xu).
[1] These authors contribute equally to this work.

https://doi.org/10.1016/j.bioactmat.2025.03.012
Received 27 August 2024; Received in revised form 14 March 2025; Accepted 14 March 2025

the treatment of osteoporosis due to they can proliferate and differentiate into osteoblastic cells under defined conditions, thus contributing to the formation of bone [7,8]. Although some progress has been achieved, some challenges such as immune rejection still exist. Thus, there is an urgent need for a safe and effective therapeutic strategy for the treatment of osteoporosis.

Exosomes are nanosized membrane vesicles actively secreted by cells, which play a crucial role in various biological processes by transferring DNA, miRNA, proteins, and other molecules between cells [9–14]. It has been widely recognized that exosomes play an important role in the regulation of bone homeostasis [15]. Studies have shown that exosomes derived from mesenchymal stem cells and osteoblasts promote osteoblastic bone formation by multiple pathways [16–18]. In addition, exosomes secreted by endothelial cells enhanced osteoblast activity and prevented the development of osteoporosis [19]. However, it is difficult to obtain a sufficient number of exosomes from these cells.

Plasma therapy is considered a promising treatment to provide antibodies and nutrition to patients. Accumulated evidence has demonstrated that young blood could reverse aging-associated impairments in older individuals [20,21]. Study on heterochronic parabiosis has demonstrated that exposure to youthful circulation restored fracture repair and enhances bone formation ability in older animals [22]. It has been shown that exosomes exist in the circulation, and their content in plasma is much higher than that of exosomes secreted by a single cell type [23]. Cheng et al. found that extracellular vehicles (EVs) from young blood reversed aged cell bioenergetics and promoted skeletal muscle regeneration, which suggesting that EVs are key mediators in restoring ageing-related damage [24]. Interestingly, the injection of EVs isolated from the serum of aged mice did not show any improvement in skeletal muscle regeneration and function.

In this study, we evaluated the therapeutic potential of exosomes derived from young and older human plasma on OVX-induced OP. Our findings demonstrated that exosomes from both young and older human plasma enhanced bone formation and reduced bone resorption. Notably, treatment with exosomes derived from young plasma (Y-EXO) resulted in superior outcome compared to treatment with exosomes from older plasma (O-EXO). miRNA sequencing and our experiments confirmed that Y-EXO improved the osteogenic differentiation ability of MSCs by encapsulating miR-142-5p. These results may provide new insights for bone damage repair and fracture prevention (Fig. 1).

2. Materials and methods

2.1. Plasma collection from healthy young and elderly human

The blood samples were selected from 5 healthy young adults aged 18–25 years and 5 healthy older adults aged 65–70 years. Collection of blood was approved by the Ethics Committee of Tongren Hospital Affiliated to Shanghai Jiao Tong University School of Medicine (2022-046-01). Informed consent was obtained from each participant. The blood samples were collected into EDTA anticoagulant tube, and plasma was obtained by centrifuging for 15 min at 4 °C at 2500 *g*. The supernatant was collected after centrifuged again at 2500 *g* for 15 min and frozen in −80 °C.

2.2. Exosomes isolation and characterizations

Exosomes isolation and characterizations were carried out as described previously [21]. The thawed plasma was centrifuged at 2000 g for 10 min and then at 12000 g for 30 min at 4 °C to remove cell debris and larger-sized vesicles. The supernatant was filtered with a 0.22 μm syringe filter (SLGPO33RB, Millipore, UA) and diluted with 3 ml PBS to reduce viscosity. The resulting plasma was ultracentrifuged at 120,000 g for 2 h at 4 °C. The obtained exosomes precipitate was suspended in 100

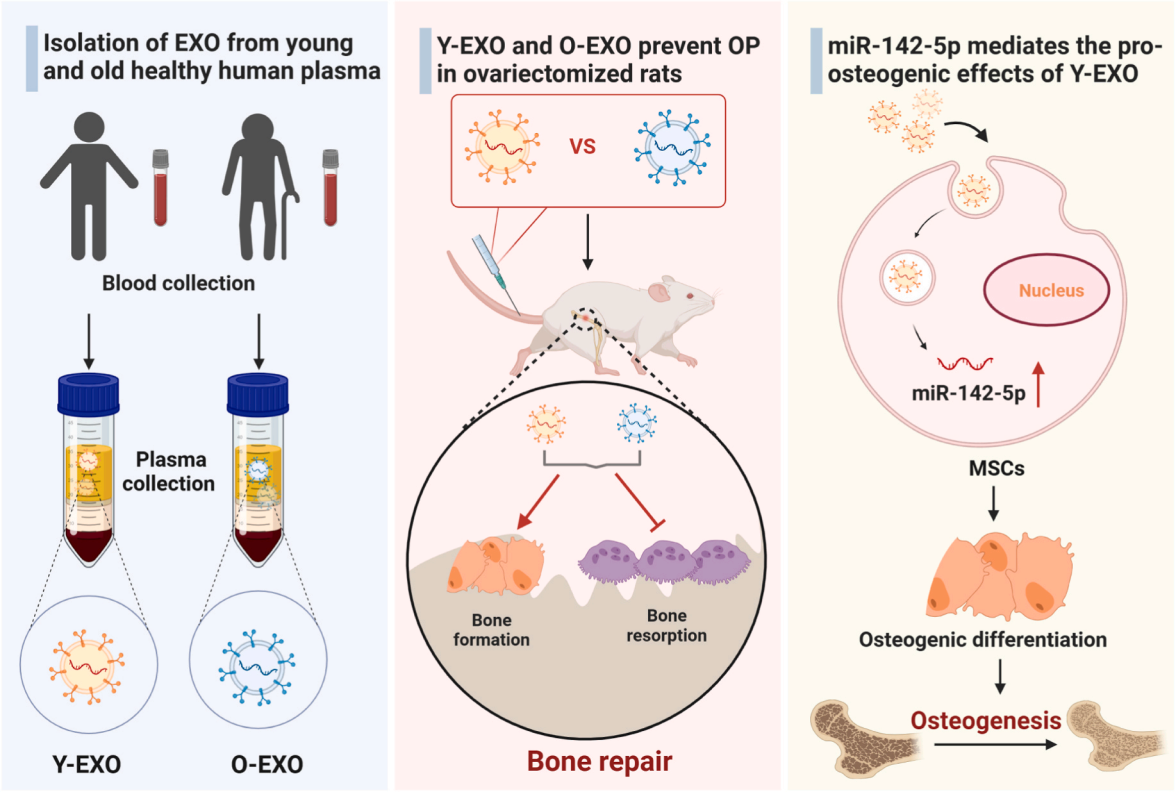

Fig. 1. Schematic illustration of the isolation of exosomes (EXO) from young and old healthy human plasma, and their functions and mechanisms for the treatment OP. Exosomes derived from young (Y-EXO) and old (O-EXO) healthy human plasma were isolated and analyzed. Both Y-EXO and O-EXO promoted bone repair in ovariectomized rats through osteogenesis promotion and osteoclast suppression. Y-EXO promoted osteogenic differentiation by transmitting miR-142-5p into MSCs.

μL PBS. Exosomes from each group were pooled together for subsequent cell and animal experiments. Transmission Electron Microscope (TEM, JEM1400FLASH, JEOL, Japan) was used to identify the morphology of exosomes. Nanoparticle tracking analysis (NTA, ZetasizerNanoZSP, US) was employed to measure exosomes diameters and concentrations. The protein content of exosomes was determined using the BCA protein assay (P0011, Beyotime, Shanghai, China). The positive markers of exosomes (CD63, CD9 and CD81) and the negative marker (calnexin) were analyzed via western blotting.

2.3. Cell culture

Human bone marrow-derived MSCs were purchased from Cyagen (Suzhou, China). MSCs were cultured in OriCell® adult BMSC complete medium (Cyagen) at 37 °C conditions with 5 % CO_2. The purity of cells ($CD45^-$, $CD34^-$, $CD44^+$ and $CD29^+$) was assessed by flow cytometry and only cells with a purity greater than 90 % were chosen for additional experiments.

2.4. Cell proliferation assays

The proliferation of MSCs cells was tested by Cell Counting Kit-8 assay (CCK-8) according to the manufacturer's instructions. In brief, cells were seeded into 96-well plates at a density of 2×10^3 cells/well and cultured in growth media at 37 °C for varying durations. Following treatment with Y-OEX and O-EXO (1×10^9/mL) for 24 h, 10 μL of CCK-8 solution was added to each well and incubated for an additional 2 h. Subsequently, the absorbance of cells (450 nm) was measured by a microplate reader.

2.5. Wound healing assay

The cell migratory capacity was observed using wound healing assays. Briefly, MSCs were grown in 6-well plates until monolayer formation and starved for 24 h in serum-free medium. MSCs were scratched with a pipet tip and cultured with Y-OEX and O-EXO (1×10^9/mL). Then, the scratched area was imaged at 0 and 24 h after scratching. Wound confluence was quantified using ImageJ.

2.6. ALP activity assay

ALP activity assay was determined using Alkaline Phosphatase Assay Kit (Abcam, ab83369). MSCs were seeded into 48-well culture plates at the density of 2.5×10^3 cells/well. The cells were then incubated with Y-OEX and O-EXO (1×10^9/mL) in osteogenic differentiation medium (containing 5.0 mM β-glycerophosphate and 50 μg/mL ascorbic acid) after cultured in growth medium. Following 14 days of culture, the cells were washed twice with deionized water and fixed with 4 % paraformaldehyde for 30 min. Cells were stained with an ALP kit for subsequent imaging. Cells were stained with an ALP kit for subsequent imaging. Furthermore, the cells were washed with ice-cold PBS and lysed with 0.2 % TritonX-100, and ALP activity was assessed using an ALP activity kit in accordance with the manufacturer's instructions.

2.7. ARS staining assay

The mineralization nodules were measured by ARS staining, a marker for the late stages of osteogenesis. MSCs were seeded at a density of 5×10^4 cells/well in 24-well culture plates. The cells were then incubated with Y-OEX and O-EXO (1×10^9/mL) in osteogenic differentiation medium (containing 5.0 mM β-glycerophosphate and 50 μg/mL ascorbic acid) after cultured in growth medium. Following a 2-week treatment, the cells were fixed with 95 % ethanol for 10 min, washed twice with PBS, stained with ARS (40 mM) for 30 min, and then washed with deionized water. Quantitative analysis of mineralized matrix nodules dissolved in 10 % (w/v) cetylpyridium chloride was performed by measuring absorbance at 570 nm wavelength.

2.8. TRAP staining assay

To measure the effects of O-EXO and Y-EXO on osteoclast activity, mouse RAW264.7 cells (5×10^4 cells/well) were seeded in 24-well culture plates with the complete medium plus M-CSF (30 ng/mL) and RANKL (50 ng/mL). After being exposed to O-EXO or Y-EXO (1×10^9/mL) for 7 days, cells were fixed with 4 % paraformaldehyde and treated with a TRAP Kit according to manufacturer's instruction. Osteoclasts were defined as TRAP-positive multinucleated cells containing more than three nuclei.

2.9. Animal experimental design

All six- to eight-month-old female SD rats were anesthetized and underwent either ovariectomy or sham operation. After surgery, the rats were allowed a four-week recovery period before their bone mineral density (BMD) was measured using microCT (Bruker micro-CT system, Germany). To investigate the bone targeting of exosomes from the plasma of healthy adults, Dio-labeled exosomes were injected into the tail vein of OVX rats, and tissues were collected after one day for immunostaining. To evaluate the anti-osteoporosis activity in vivo with exosomes from plasma of young and older healthy adults, the rats were intravenously injected with 0.5 mL PBS (PBS control group) or 2×10^{10} Y-EXO or O-EXO in 0.5 mL PBS at day 1, day 8, day 15, and day 22 following OVX.

2.10. Ex vivo imaging

Cy5-labeled Y-EXO was administered intravenously (i.v.) to C57BL/6 mice. The mice were euthanatized at different time points (1 d, 3 d, 7 d, and 14 d) and the bone tissues were harvested for ex vivo imaging.

2.11. Blood collection and serum analysis

OVX rats were euthanized at 4 weeks after surgery, and blood were collected. For obtaining serum, the blood was allowed to clot at room temperature for 30–60 min and then centrifuged for 15 min at 2000 g at 4 °C. The supernatant serum was collected and used for analysis. Serum levels of TRACP-5b (E-EL-R0939, Elabscience) and osteocalcin (NBP2-68153, Novus) were measured by ELISA kits.

2.12. Micro-CT analyses

The femur bones isolated from the female OVX rats treated with Y-EXO or O-EXO were scanned and analyzed using a micro-CT system (Bruker micro-CT system, Germany).

2.13. MiRNA transfection

MiR-142-5p mimic and non-targeting control miRNA (miR-NC) were synthesized by Sangon (Shanghai, China). The sequence of miR-25-3p mimic was 5′-CAUAAAGUAGAAAGCACUACU-3′. MiR-142-5p inhibitor was purchased from RiboBio Co., LTD (Guangzhou, China). Cells were transfected with 2 μg of miR-142-5P mimic, miR-142-5p inhibitor or miR-NC in six-well plates using a commercial transfection reagent lipofectamine 2000 (Invitrogen) according to the manufacturer's instructions. After 48 h of transfection, the miRNA expression was confirmed by real-time fluorescence quantitative PCR (qRT-PCR) analysis.

2.14. Real-time fluorescence quantitative PCR

Real-time fluorescence quantitative PCR was conducted to assess the mRNA expression levels of osteogenic genes and miR-142-5p. MSCs

were transfected with miR-142-5p mimics, miR-142-5p inhibitor or non-targeting control miRNA (miR-NT) oligos for 48 h. Total RNA was extracted using Trizol reagent (Invitrogen) following the manufacturer's instructions. To obtain cDNA, 2 μg of total RNA was used as a template and reverse transcribed into cDNA using the PrimeScript RT reagent Kit (RR067A, Takara). The resulting cDNA was used for qRT-PCR analysis using SYBR-green Premix Ex TaqTM (RR420A, Takara) according to manufacturer's instructions. The relative target gene expression was calculated using the $2^{-\Delta\Delta CT}$ method, with normalization to β-actin or U6 levels in all samples.

Gene	Primer sequence (5′-3′)
miR-142-5p	AGCGAGGCCATAAAGTAGAAA
OCN	GCTGTTTGTTCGGGTCTC
COLA1	CAGAGGCGAAGGCAACA
β-actin	GATGGTGGGAATGGGTCAGAAGG

2.15. Statistical analysis

All statistical analyses were carried out using GraphPad Prism 8.0 software (GraphPad Software, Inc). Group comparisons were conducted using the two-tailed independent Student's t-test. When comparing more than two groups, one-way analysis of variance (ANOVA) and Tukey's post-hoc test was employed. The data are presented as means ± SD unless otherwise indicated. $P < 0.05$ was considered statistically significant.

3. Results

3.1. Characterization of exosomes derived from young and older human plasma

The exosomes from young and older volunteers' plasma were isolated by ultrahigh-speed gradient centrifugation. The expression of exosome-positive biomarkers CD9, CD63, and CD81 and the exosome-negative biomarker calnexin, was assessed using a Western blot assay. As shown in Fig. 2A, CD9, CD63, and CD81 were expressed in exosomes from both young and older individuals (Y-EXO and O-EXO), while calnexin, an endoplasmic reticulum marker, was not detected. Nanoparticle tracking analysis (NTA) further confirmed that the mean diameter of the obtained exosomes was 90–120 nm (Fig. 2B). The morphology of the exosomes was assessed using transmission electron microscopy (TEM). As shown in Fig. 2C, both Y-EXO and O-EXO exhibited a circular, double-layered vesicle structure. These results demonstrated that exosomes were successfully extracted and purified.

3.2. Exosomes from young and older human plasma promote osteogenesis and inhibit osteoclastogenesis

Osteoblasts are the main cells involved in bone formation, which are responsible for synthesis, deposition, and mineralization of bone matrix [25]. MSCs can differentiate into osteoblasts under specific conditions, playing a major role in bone regeneration and remodeling [26–28]. Therefore, we investigated the effects of Y-EXO and O-EXO on the proliferation, migration and mineralization of MSCs. Flow cytometry was initially used to detect the characteristics of MSCs (as $CD45^-$, $CD34^-$, $CD44^+$ and $CD29^+$). The results showed that the purity of the resulting population exceeded 98 % for $CD45^-$ $CD34^-$ and 97 % for $CD29^+$ $CD44^+$ (Fig. S1). As shown in Fig. 2D, both Y-EXO and O-EXO promoted the proliferation of MSCs. However, Y-EXO treatment exhibited a better effect than O-EXO treatment. The migration capacity of MSCs after exosome treatment was further tested using the scratch assay. Comparison to O-EXO, Y-EXO significantly increased MSCs migration (Fig. 2E and S2). Alkaline phosphatase (ALP) is an early marker of osteogenesis, and its expression levels indicate the formation of bioactive bone [29]. As shown in Fig. 2F and G, ALP activity was increased by both O-EXO and Y-EXO compared to untreated osteoblastic cultures. Interestingly, significantly greater ALP activity was observed in the treatment with Y-EXO compared to those with O-EXO (Fig. 2F and G). Extracellular matrix (ECM) mineralization was used as a marker of osteogenic differentiation. Alizarin red staining (ARS) was used to further measure the formation of calcified nodules, and both exosomes increased the deposition of calcium compared to the control. More matrix nodules were formed when treated with Y-EXO, which was consistent with that of ALP staining (Fig. 2H and I). Bone remodeling requires a dynamic equilibrium between bone formation mediated by osteoblasts and bone resorption mediated by osteoclasts [30]. Abnormal osteoclast differentiation and activity has been considered primary causes of osteoporosis [31,32]. Tartrate-resistant alkaline phosphatase (TRAP) is marker of osteoclast, usually elevated in osteoclasts [33]. We then measured osteoclast numbers by TRAP staining and observed a significant decrease in the number of osteoclasts with the treatment of both exosomes. In addition, significantly fewer osteoclast were detected in Y-EXO treatment than O-EXO (Fig. S3), indicating the superior ability of Y-EXO in promoting osteogenesis and suppressing of osteoclastogenesis.

3.3. Exosomes from young and older human plasma increase bone mass in OVX-induced osteoporotic rats

In order to fully evaluate the therapeutic effect of exosomes from young and older human plasma, we first investigated the delivery of exosomes to bone after intravenous administration. Exosomes were first stained with Dio before being injected into rat models via tail veins. Surprisingly, we found that the exosomes could effectively accumulate in bone tissue (Fig. 3A). The bone distribution and retention in of Y-EXO in C57BL/6 mice at various time points were observed by the ex vivo imaging system. As shown in Fig. S4A and C, Y-EXO were significantly clustered at the site of osteoarticular on day 1. A significant decrease in the fluorescence intensity was observed on day 7, but it returned to near-normal on the day 14 (Figs. S4A and B). To study the therapeutic effects of injected Y-EXO and O-EXO on osteoporosis, an osteoporosis rat model was established by ovariectomy (OVX). Four weeks after ovariectomy, female rats were randomly divided into four groups: a sham-operated control group (Healthy), an ovariectomized group (OVX), an ovariectomized group treated with Y-EXO (Y-EXO), and an ovariectomized group treated with O-EXO (O-EXO). The proximal tibiae were harvested and scanned using ex vivo micro-computed tomography (Micro-CT). Bone microstructural parameters were accurately displayed in CT (Fig. 3B). As shown in Fig. 3C–E, we found that bone mineral density (BMD), trabecular bone volume (BV/TV), and trabecular thickness (Tb.Th) were greater in both the O-EXO and Y-EXO groups compared to the OVX group. Interestingly, the use of Y-EXO led to higher BMD, BV/TV and Tb.Th compared with the use of O-EXO. Consistent with these results, the H&E images showed that OVX surgery induced significant bone loss. Osteoporotic rats treated with Y-EXO and O-EXO showed increased trabecular number and density, with Y-EXO treatment further enhancing these outcomes (Fig. 3F).

3.4. Exosomes from young and older human plasma promote bone formation and inhibit bone resorption

Osteoprotegerin (OPG) is a secreted protein that inhibits osteoclastic activity, and increased OPG expression can reflect osteogenic ability [34]. We showed that OPG expression was significantly decreased in OVX-induced osteoporotic rats, but treatment with both Y-EXO and O-EXO maintained OPG expression compared to OVX group (Fig. 4A). The number of OPG-positive cells was counted using software, and the results indicate that the number of OPG-positive cells in Y-EXO group was higher than in the O-EXO group, indicating Y-EXO had a better pro-osteogenic ability than O-EXO (Fig. 4C). Furthermore, our

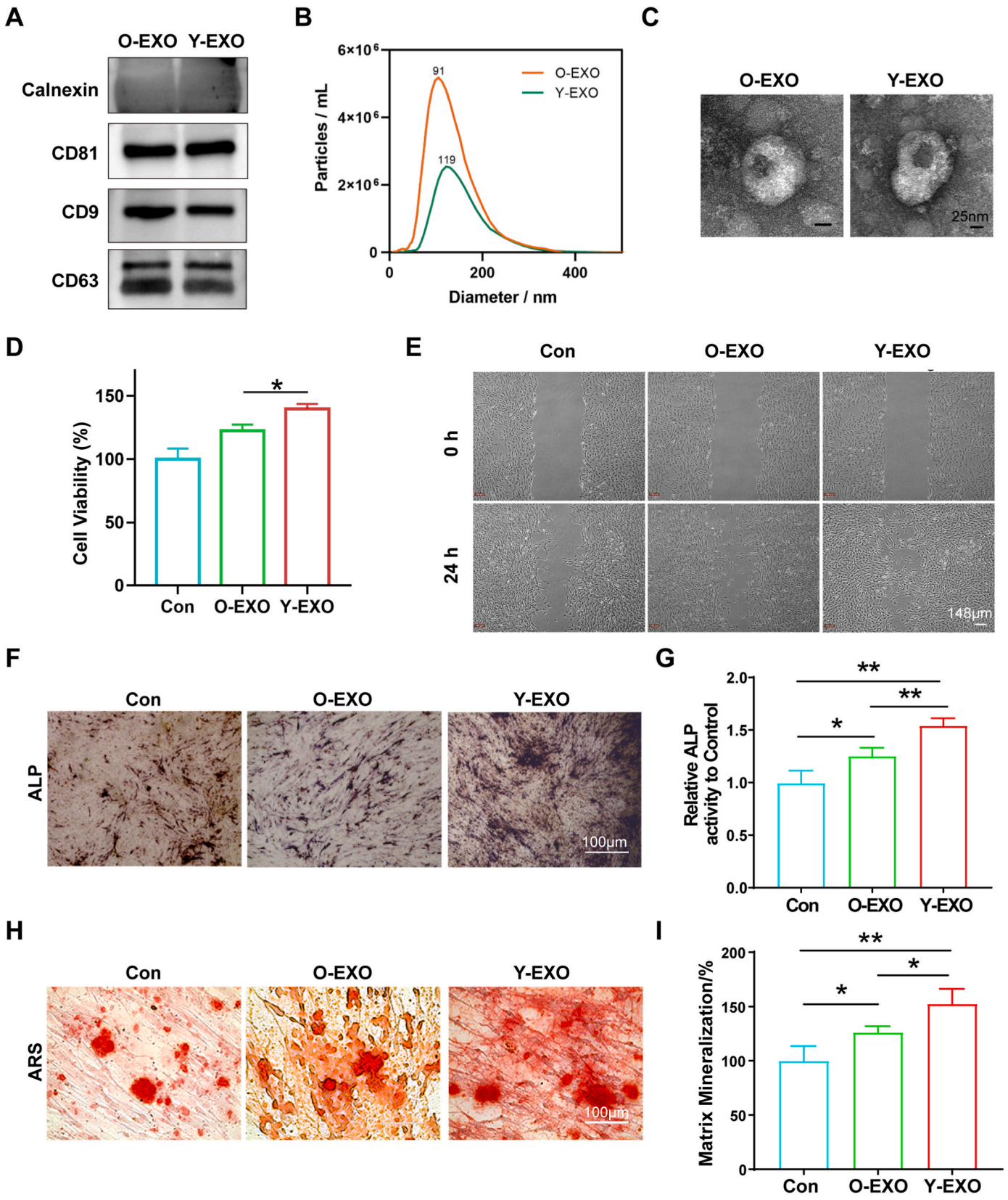

Fig. 2. Characterization of Y-EXO/O-EXO and the pro-osteogenic properties of Y-EXO/O-EXO in vitro. (A) The expression of CD9, CD63, CD81, and calnexin in Y-EXO and O-EXO. (B) Zeta potential of Y-EXO and O-EXO. (D) Cell proliferation for MSCs incubated with Y-EXO or O-EXO. (C) Transmission electron microscopy imaging of Y-EXO and O-EXO (Scale bars = 25 nm). (D) Cell viability for MSCs incubated with Y-EXO or O-EXO. (E) Representative images of the migration of MSCs across a scratch after incubation with Y-EXO or O-EXO (Scale bar = 148 μm). (F) ALP activity and (H) Alizarin Red S staining of MSCs after incubation with Y-EXO or O-EXO (Scale bar = 100 μm). Quantification of (G) relative ALP activity, and (I) the amount of Alizarin Red S that stained the mineralized matrix. Data are expressed as mean ± SD (n = 3, $*p < 0.05$, $**p < 0.01$ and $***p < 0.001$).

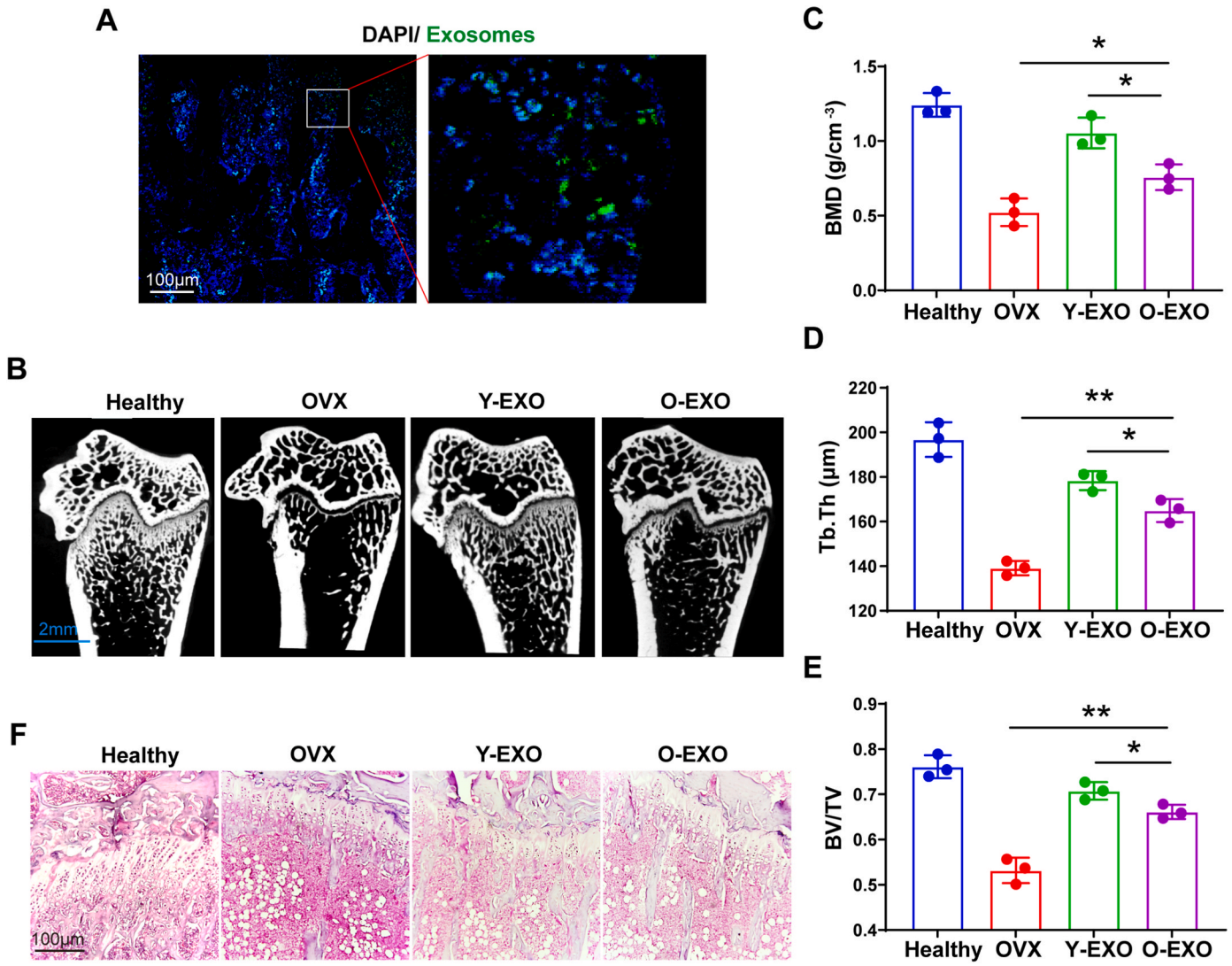

Fig. 3. Y-EXO and O-EXO targets the bone and increases bone mass of OVX-induced osteoporotic rats in vivo. (A) Confocal imaging of Y-EXO or O-EXO in massive bone at day 1 after infusion. (B) After 4 weeks of treatment, the femurs from rats in each group were harvested, and the distal femur was scanned using micro-CT. (C–E) Quantitative results of (C) BMD changes and some trabecular parameters, including trabecular bone volume expressed as percentage of (D) trabecular thickness (Tb.Th) and (E) total tissue volume (BV/TV). (F) Photomicrographs of bone sections stained by H&E. Data are expressed as mean ± SD (n = 3, $*p < 0.05$, $**p < 0.01$).

tartrate-resistant acid phosphatase (TRAP) staining results showed that TRAP-positive cells increased after OVX surgery. However, treatment with either O-EXO or Y-EXO strongly decreased the numbers of TRAP-positive cells in the bone tissue of OVX rats. Y-EXO group exhibited lower TRAP expression compared with O-EXO group (Fig. 4B and D). Tartrate-resistant acid phosphatase 5b (TRACP 5b) is a bone resorption marker and increased levels of serum TRACP 5b is likely to be associated with increased osteoclast activity [35,36]. Changes in serum TRACP 5b levels were consistent with TRAP staining results, showing that exosome treatment markedly decreased serum levels of TRACP-5b, which were lower in the O-EXO group compared to the Y-EXO group (Fig. 4E). We also tested the levels of a specific bone formation markers, osteocalcin, in the serum of rats. The serum levels of osteocalcin were significantly increased in Y-EXO-treated osteoporotic rats compared to O-EXO treatment and healthy group (Fig. 4F). Taken together, these results indicated that exosomes from both young and older human plasma could enhance bone formation and reduce bone resorption, with Y-EXO treatment producing a superior outcome compared to O-EXO treatment.

3.5. MiR-142-5p is upregulated in exosomes derived from young healthy man plasma and promotes MSCs osteogenic differentiation

MicroRNAs (miRNAs) are abundantly present in exosomes and play a crucial role in bone formation and bone resorption [37]. To further investigate the mechanism of Y-EXO-induced osteogenesis, we performed miRNA sequencing on exosomes isolated from young and older human plasma. The miRNA sequencing results indicated significant differences in the miRNAs carried by exosomes derived from young man compared to those from old controls. In total, 31 miRNAs were identified as being up-regulated in Y-EXO compared with O-EXO, while 17 miRNAs were identified as being down-regulated (Fig. 5A). Interestingly, we observed that miR-142-5p was significantly elevated in Y-EXO, indicating that exosomal miR-142-5p may play a very important role in Y-EXO-mediated bone regeneration (Fig. 5A and B). To explore the role of miR-142-5p in osteoblast differentiation, we first constructed a miR-142-5p mimic. qRT-PCR analysis suggested that miR-142-5p expression was considerably upregulated when the cells were transfected with miR-142-5p mimic (Fig. S5). ALP is commonly used as a marker for early-stage osteogenic differentiation whereas osteocalcin (OCN) serves as an indicator for late-stage osteogenic differentiation

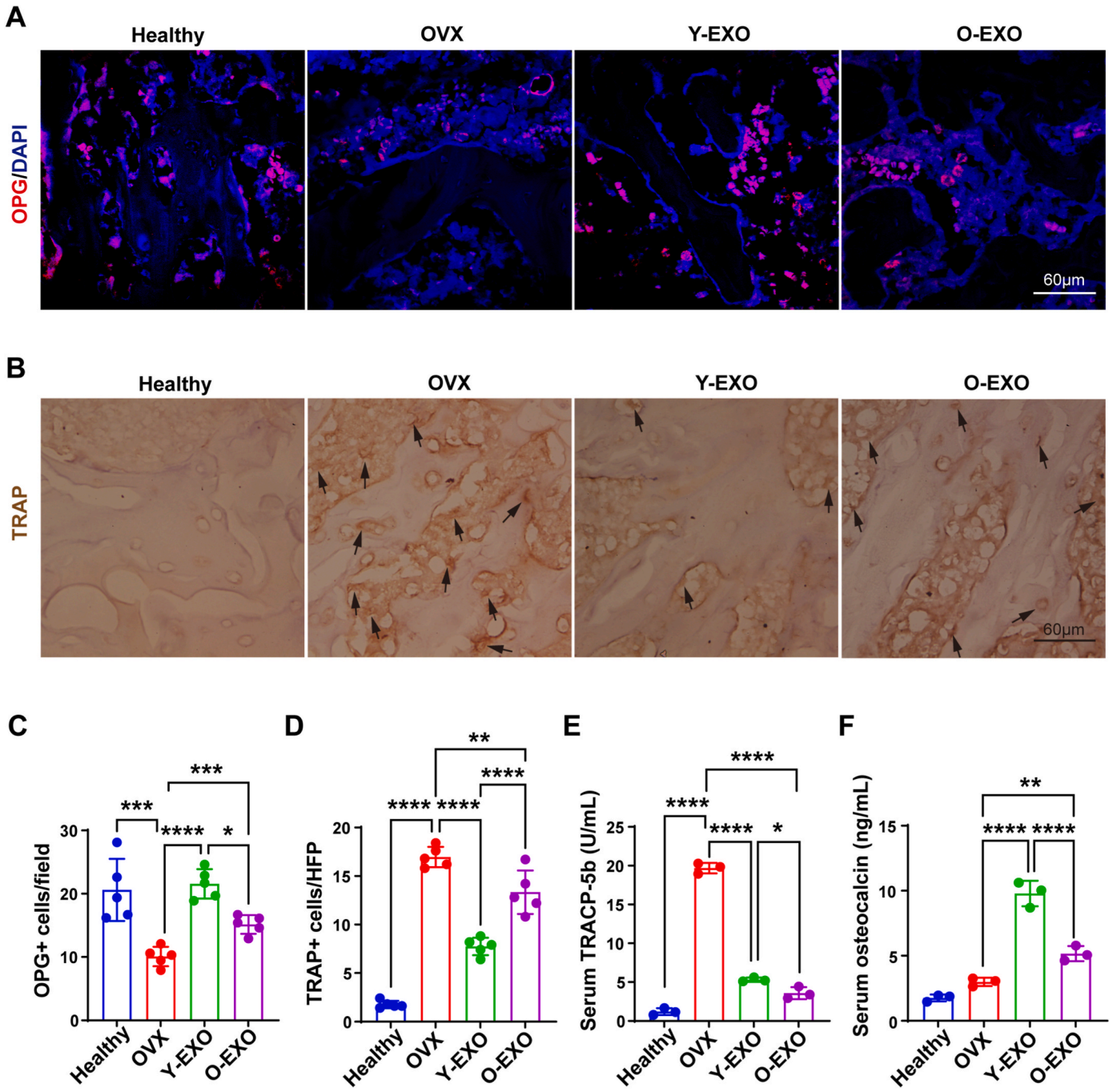

Fig. 4. Y-EXO and O-EXO promotes bone formation and inhibits bone resorption. (A) Detection of OPG after Y-EXO and O-EXO treatment and (C) their quantitative results. (B) TRAP staining showing the osteoclasts and (D) their quantitative results. Data are expressed as mean ± SD (n = 5). (E) Detection of serum TRACP-5b and (F) osteocalcin level after Y-EXO and O-EXO treatment. Data are expressed as mean ± SD (n = 3, $^{*}p < 0.05$, $^{**}p < 0.01$, $^{***}p < 0.001$, and $^{****}p < 0.0001$).

[38,39]. Therefore, we examined the mRNA levels of ALP and OCN in MSCs transfected with miR-142-5p mimic. As shown in Fig. 5C and S6, transfection of miR-142-5p mimic significantly increased the gene expression levels of ALP and OCN. To further explore the effect of miR-142-5p on MSCs osteogenic differentiation, we performed bone differentiation induction and transfected cells with miR-142-5p mimic. The ALP staining assay showed that miR-142-5p significantly increased ALP activity compared to cells transfected with a non-targeting control miRNA mimic (Fig. 5D and F). Consistent with the results of the ALP staining assay, the ARS staining assay showed that miR-142-5p significantly increased extracellular calcium deposits (Fig. 5E and G). Silencing of miR-142-5p prevented osteogenic differentiation of MSCs, consistent with the results of the miR-142-5p overexpression experiments (Fig. 6). In addition, transfection of miR-142-5p mimic significantly promoted MSCs proliferation as compared with MSCs transfected with non-targeting control miRNA mimic (Fig. 5H). Taken together, these results suggested an essential involvement of miR-142-5p in the process of bone formation.

3.6. *miR-142-5p mediates the pro-osteogenic effects of exosomes from young healthy man plasma*

To explore whether miR-142-5p is involved in the Y-EXO-driven osteogenesis, a miRNA-142-5p inhibitor was applied to downregulate

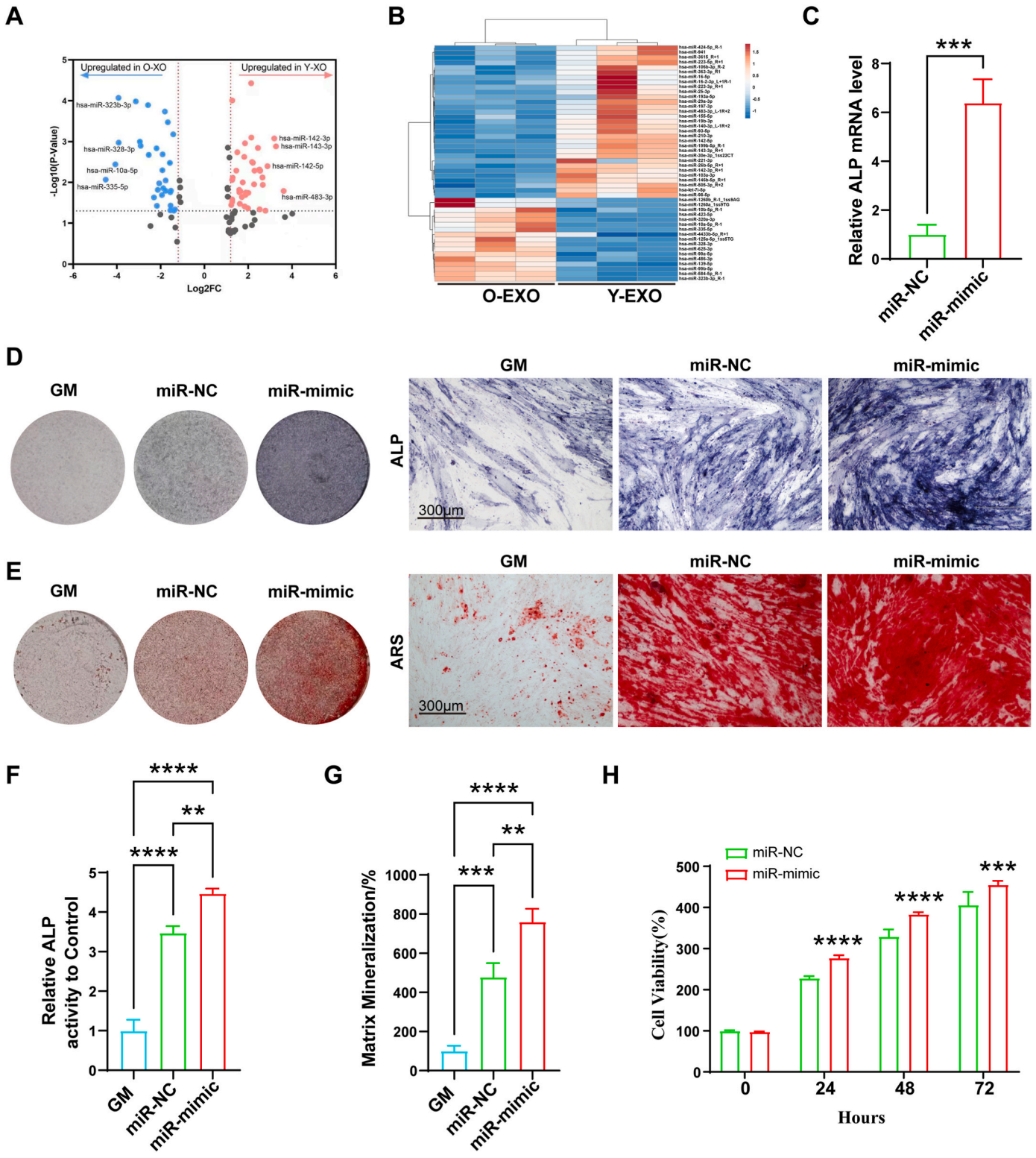

Fig. 5. miR-142-5p mimics the effect of young plasma-derived exosomes on bone formation in vitro. (A) The volcano plot analysis of the differential expressed miRNAs in Y-EXO and O-EXO. (B) Heatmap clustering analysis of the differentia expression of miRNAs in Y-EXO and O-EXO. (C) The mRNA expression levels of ALP in MSCs transfected with miR-142-5p mimic. (D) ALP activity staining of MSCs incubated with growth medium (GM), or osteogenic medium with miR-142-5p mimic. (E) Alizarin Red S staining of MSCs incubated with growth medium (GM), or osteogenic medium with miR-142-5p mimic. Quantifying (F) relative ALP activity and (G) the amount of Alizarin Red S that stained the mineralized matrix. (H) Cell proliferation for MSCs transfected with miR-142-5p mimic or non-targeting control miRNA mimic (miR-NC). Data are expressed as mean ± SD (n = 3, $^{**}p < 0.01$, $^{***}p < 0.001$, $^{****}p < 0.0001$).

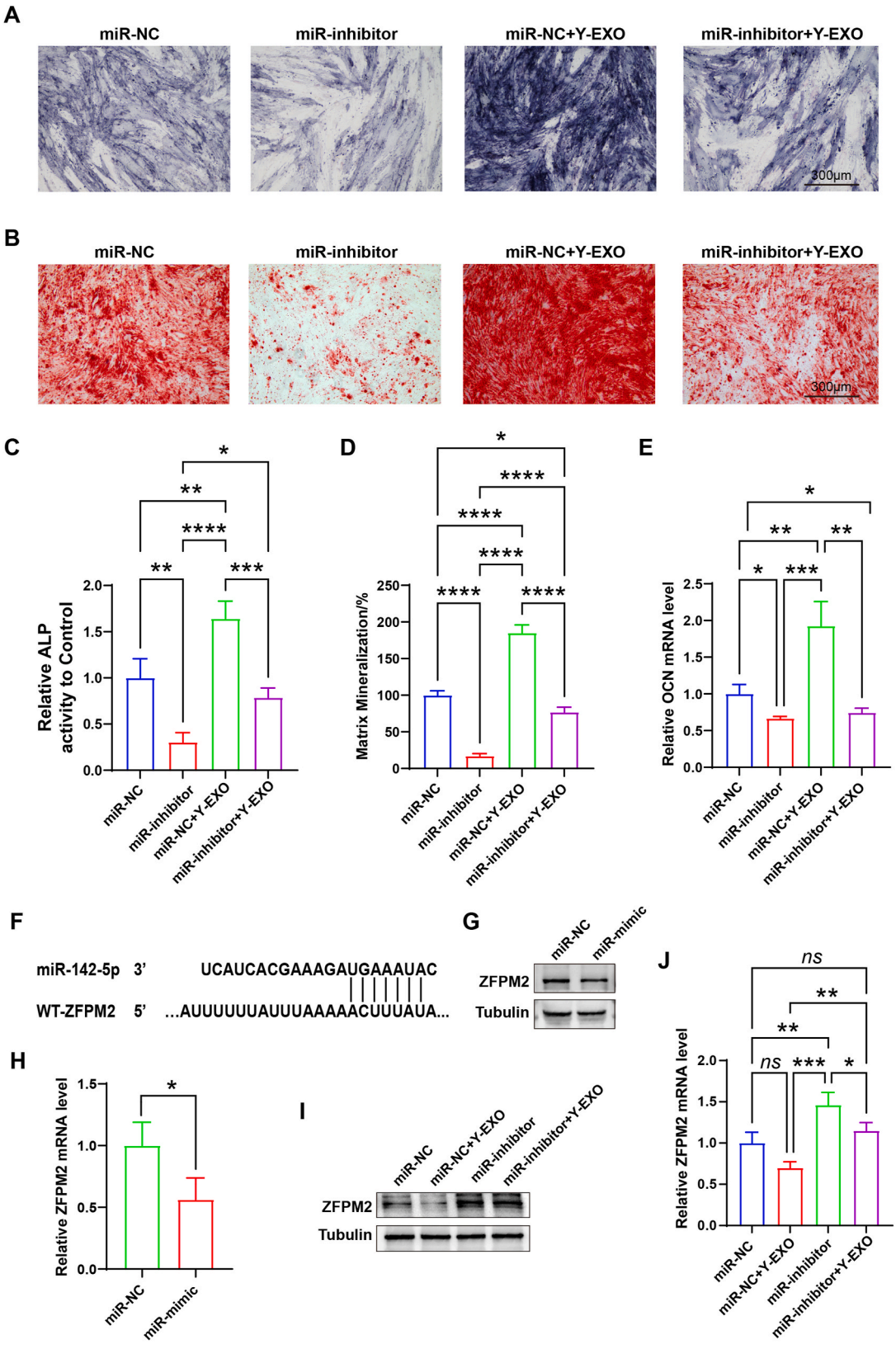

Fig. 6. MiR-142-5p in young plasma-derived exosomes regulates osteogenesis via targeting ZFPM2. (A) ALP activity staining of MSCs transfected with miR-142-5p inhibitor under Y-EXO treatment. (B) Alizarin Red S staining of MSCs transfected with miR-142-5p inhibitor under Y-EXO treatment. Quantification of (C) relative ALP activity and (D) the amount of Alizarin Red S that stained the mineralized matrix. (E) The mRNA expression levels of OCN in MSCs transfected with miR-142-5p inhibitor under Y-EXO treatment. (F) The putative binding site for miR-142-5p is located in the 3′-UTR region of ZFPM2 mRNA. (G) Results of ZFPM2 protein levels in MSCs transfected with the miR-142-5p mimic. (H) Results of ZFPM2 mRNA levels in MSCs transfected with the miR-142-5p mimic. (I) Results of ZFPM2 protein levels in MSCs after transfection with miR-142-5p inhibitor and Y-EXO treatment. (J) Results of ZFPM2 mRNA levels in MSCs after transfection with miR-142-5p inhibitor and Y-EXO treatment. Data are expressed as mean ± SD (n = 3, $^{*}p < 0.05$, $^{**}p < 0.01$, $^{***}p < 0.001$, $^{****}p < 0.0001$).

the expression of miR-142-5p (Fig. S7). The ALP activity was examined to evaluate the osteogenic activity in MSCs treated with Y-EXO after transfection with the indicated inhibitor. As shown in Fig. 6A, C and S8A, Y-EXO significantly elevated ALP staining and activity in MSCs, which was markedly attenuated by silencing miRNA-142-5p. The role of miR-142-5p in the pro-osteogenic ability of Y-EXO was further evaluated by alizarin red staining. As shown in Fig. 6B, D and S8B, miR-142-5p silencing inhibited the mineralization ability of BMSCs induced by Y-EXO. Meanwhile, mRNA expression levels of osteoblast marker genes, OCN, significantly decreased in MSCs transfected with the miR-142-5p inhibitor under Y-EXO treatment (Fig. 6E). Taken together, miRNA-142-5p exerted an essential regulatory effect on osteoblast differentiation of MSCs induced by Y-EXO.

3.7. MiR-142-5p regulates MSC osteogenic differentiation via ZFPM2

To further determine the underlying molecular mechanisms by which miR-142-5p promotes MSCs osteogenesis, we used the online databases TargetScan (https://www.targetscan.org/mamm_31/) and miRDB (https://mirdb.org/mirdb/index.html) to predict the potential downstream target genes of miR-142-5p. ZFPM2 was predicted by both databases to be a downstream target of miR-142-5p. Furthermore, previous study indicated that ZFPM2 is a negative regulator for osteogenesis [40]. Therefore, our study concentrated on exploring the connection between miR-142-5p and ZFPM2. The interaction model between miR-142-5p and the 3′UTR of ZFPM2 was shown in Fig. 6F. Subsequently, we assessed the effect of miR-142-5p overexpression on the expression of ZFPM2 by Western blot analysis and RT-qPCR. As shown in Fig. 6G and H, the protein and mRNA levels of ZFPM2 were significantly decreased by miR-142-5p overexpression. In addition, Y-EXO significantly reduced the levels of ZFPM2 protein and mRNA, which could be reversed by miR-142-5p inhibitor (Fig. 6I and J). These results suggested that exosome miR-142-5p regulated osteogenesis by targeting ZFPM2.

4. Discussion

OP is a chronic and systemic metabolic bone disease characterized by low bone mass and the degradation of bone microarchitecture, leading to an increased risk for fragility fractures [41]. The effectiveness of many drugs used to treat OP is limited by their toxicity or low bioavailability [4,42]. Thus, effective therapies are urgently needed for OP patients. We found that both exosomes from young and older human plasma could reverse osteoporosis by promoting bone formation and inhibiting bone resorption. It is worth noting that exosomes from young healthy human plasma showed a more optimal therapeutic effect. Furthermore, our results indicated that the regulatory role of exosomes in osteoblast formation is mediated through miR-142-5p.

Heterochronic blood exchange (HBE) has demonstrated that young blood or plasma exerts robust protective effects against aging and age-related diseases including alzheimer's disease, cerebrovascular diseases, bone, liver and adipose tissue [24,43–45]. These effects involve the restoration of autophagy, enhanced neurogenesis, and reduction in oxidative stress, inflammation, and apoptosis [46,47]. However, blood plasma contains complex components, encompassing various circulating factors, proteins, and other components. The mediators contributing to anti-aging effects remain poorly defined. Exosomes, carrying various cargo molecules including DNA, RNA, lipids and proteins, are widely present in the blood, serving as mediators for the exchange of substances between cells. Sahu et al. reported circulating extracellular vehicles (EVs) are a major effector in restoring aged cell bioenergetics and promoting skeletal muscle regeneration in response to young serum [24]. We previously showed that exosomes from the plasma of young human cloud reduce brain injury and cell ferroptosis after intracerebral hemorrhage (ICH), and then promote functional recovery [23]. In the present study, we found that exosomes isolated from the plasma of young and old healthy individuals prompted MSCs proliferation and migration in vitro. Additionally, the in vitro and in vivo experiment suggested that exosomes from both age groups could restore the osteogenic ability of MSCs, inhibit osteoclast formation and ameliorate the OP symptoms. Notably, the therapeutic effect of young adults-derived exosomes was better than that of older healthy individuals-derived exosomes. However, the anti-osteoporotic effect of exosomes isolated from the human plasma was investigated using rat model, while valuable for studying bone metabolism, may not fully replicate human physiological conditions. It has been proved in previous studies that multiple cell-derived exosomes could promote osteogenesis and inhibit bone resorption to ameliorate bone-implant osseointegration, including endothelial cell, mesenchymal stem cell, myoblast, vascular endothelial cells [19,48–52]. Nevertheless, others have shown that osteoclast-derived exosomes and M1 macrophage-derived exosomes resulted in acceleration of bone loss in osteoporosis [53]. These exosomes can be transported throughout all parts of the body with the blood circulation system to participate in cellular interactions. Further researches are needed to determine which cell-derived exosomes in plasma predominantly mediate these phenotypes. Furthermore, ex vivo imaging of Y-EXO labeled with the Cy5 fluorescent dye revealed their ability to distribute within bone tissue. The fluorescence signal persisted until day 7 and gradually diminished to baseline by day 14, aligning with previous findings. However, besides bone tissue, plasma-derived exosomes were also detected in the liver and spleen, suggesting a non-specific distribution pattern [54,55]. This implies that surface modifications of these exosomes could be a promising strategy to enhance their targeting efficiency and optimize their therapeutic potential.

The therapeutic effect of exosomes is related to the component derived from their parental cells, including miRNAs, mRNAs, and proteins [56–59]. miRNAs are a short non-coding RNA that modulate gene expression at a post-transcriptional level by binding to specifical mRNAs [60–63]. miRNAs are important in controlling osteoblast differentiation and involved in the progression of osteoporosis [64]. In order to uncover the mechanism behind the anti-osteoporotic effects of exosomes isolated from the plasma of young and old healthy man, we conducted miRNA sequencing. Sequencing analysis confirmed that the gene expression levels of miR-142-5P in young human plasma-derived exosomes were elevated compared to those of miRNA detected from old human plasma-derived exosomes. Study has shown that miR-142-5p expression was lower in the callus of aged mice than that in the callus of young mice, which directly correlated with bone healing delay associated with aging. Transfection with agomir-142-5p could elevate osteoblast activity and promote matrix mineralization in MC3T3-E1 cells. Injection of agomir-142-5p into the fracture site of 18-month-old mice after fracture promoted bone formation and fracture repair [65]. Moreover, Zhao et al. found that the upregulation of mmu-miR-142-5p through transfection of exogenous agomiR-142-5p significantly increased the expression levels of osteogenic genes ALP, RUNX2 and osteocalcin (OC) in osteoblasts, indicating that mmu-miR-142-5p possesses potential for promoting bone formation [66]. Autogenous oxygen-releasing nano-bionic scaffolds was proved to have a significant pro-osteogenic effect in bone marrow mesenchymal stem cells (BMSCs). However, the combination of miR-142-5p mimics with autogenous oxygen-releasing nano-bionic scaffolds further increased osteogenic transformation at bone defects, and promoted bone healing. The potential mechanism of action was though the regulation of BMP-9 [67]. In addition, the researchers have found that Circ_0006873 enhances PTEN expression by sponging miR-142-5p, thereby regulating the Akt signaling pathway to suppress osteoblastic differentiation. This suggested a positive regulatory role of miR-142-5p in osteogenic differentiation [68]. However, Du et al. reported that miR-142-5p inhibited BMSCs osteogenic differentiation by inhibiting Lhx8 [69]. Therefore, we aimed to further explore the function of miR-142-5p in OP. In our study, transfection with miRNA-142-5p mimic into MSCs significantly upregulated the expression of osteogenesis-related genes including OCN and ALP, promoted ALP

activity and formation of mineralized nodules. However, silencing miR-142-5p showed the opposite effects compared to its overexpression. The pro-osteogenic effects of miR-142-5p in vivo need further investigation. Here, we found that ZFPM2 may be a potential downstream target of miR-142-5p. Previous studies have reported that silencing ZFPM2 promoted osteoblast differentiation [40]. It suggests that miR-142-5p may promote osteogenic differentiation of MSCs by targeting ZFPM2. However, additional experimental validation, such as a dual-luciferase reporter assay, is needed to further elucidate the regulatory mechanism of miR-142-5p on ZFPM2. Notably, Lou et al. reported that miR-142-5p promotes osteoclast differentiation in bone marrow-derived macrophages via the PTEN/PI3K/AKT/FOXO1 pathway, suggesting that Y-EXO may inhibit osteoclastogenesis through alternative mechanisms [70]. While exosomal miRNAs have the potential to regulate osteogenic and osteoclast differentiation, the underlying molecular mechanisms are typically distinct, as these processes involve two different cell types. Further research into the role of miR-142-5p in osteoclast formation will provide deeper insights into the anti-osteoporotic effects of Y-EXO.

MiRNAs are principal constituents of exosomes and play a major role in their biological function [71]. Many studies have shown that exosomes regulate the processes of bone formation and bone resorption in miRNA-dependent manners. For example, Wang et al. revealed that miR-140-3p derived from exosomes of normal BMSCs could effectively accelerate diabetic wound healing by promoting bone regeneration [72]. A previous study identified exosomal miR-217-5p as a critical factor contributing to osteoprotective effects, with inhibition of miR-217-5p reducing the function of exosomes in alleviating osteoporosis [73]. However, Xu et al. demonstrated that miR-128-3p was significantly upregulated in exosomes derived from aged MSCs and functions as a suppressor in the process of osteogenesis [74]. Likewise, miR-31a-5p was reported to be highly expressed in exosomes derived from BMSCs of aged rats, promoting osteoclastogenesis and bone resorption. In addition, Zhai et al. found that osteogenesis-related miRNAs (miR-146a-5p, miR-503–5p, miR-483-3p and miR-129-5p) and anti-osteogenic miRNAs (Hsa-miR-32-5p, Hsa-miR-133a-3p, and Hsa-miR-204-5p) exited in exosomes derived from MSCs, which regulated bone regeneration by activating the PI3K/Akt and MAPK signaling pathways [75]. Our miRNA sequencing data showed that multiple miRNAs were upregulated in Y-EXO compare to those derived from O-EXO. In addition, our results from in vitro experiments indicated that the pro-osteogenic effect induced by Y-EXO was predominantly attributed to the overexpression of miR-142-5p, but not all, indicating the involvement of other miRNAs in this process. Apart from miRNAs, protein and lipids are also the key components of exosomes, but they may not the primary contributors to the anti-osteoporosis effect of exosomes. A study on the proteomics and lipidomics of exosomes derived from three different cell types found that the protein composition of exosomes depends on their cell origin, as exosomes from different cancer cell lines shared similar proteins, in contrast to those derived from MSCs. The lipid composition of exosomes was most strongly associated with their yield and size, with exosomes derived from cells producing smaller quantities and sizes being enriched in similar lipids [76]. However, plasma exosomes derived from healthy individuals appear to have similar source and size, suggesting that the protein and lipid may not be the most critical ingredients for their therapeutic functions. Therefore, this study focused solely on the effect of miRNAs on osteoporosis, and further research is needed to investigate the roles of other components in exosomes.

5. Conclusion

In conclusion, these results demonstrate that exosomes derived from both young and old human plasma alleviate osteoporosis symptoms by promoting osteogenesis and inhibiting osteoclastogenesis. Notably, exosomes from young plasma exhibit superior therapeutic efficacy compared to those from older plasma. These pro-osteogenic effects of young plasma exosomes are mediated by miR-142-5p, which is expressed at higher levels in young plasma exosomes than in their older counterparts. MiR-142-5p may enhance bone repair by inhibiting ZFPM2 expression. Therefore, exosomes derived from healthy human plasma, particularly those from young plasma, hold promise as a novel therapeutic strategy for osteoporosis treatment.

CRediT authorship contribution statement

Zhikun Li: Writing – original draft, Validation, Methodology, Investigation, Formal analysis, Data curation. **Qifeng Yu:** Writing – original draft, Methodology, Investigation, Formal analysis, Data curation. **Xiang Cui:** Writing – original draft, Methodology, Investigation, Formal analysis, Data curation. **Yi Wang:** Methodology, Investigation, Data curation. **Ruijun Xu:** Methodology, Investigation, Data curation. **Renjie Lu:** Methodology, Investigation, Data curation. **Jiahao Chen:** Methodology, Investigation, Data curation. **Xiaohan Zhou:** Methodology, Investigation, Data curation. **Chi Zhang:** Writing – review & editing, Project administration, Conceptualization. **Lanya Li:** Writing – review & editing, Project administration, Funding acquisition, Conceptualization. **Wei Xu:** Writing – review & editing, Supervision, Project administration, Funding acquisition, Conceptualization.

Ethics approval and consent to participate

The animal experiments were approved by the Ethics Committee of Tongren Hospital Affiliated to Shanghai Jiao Tong University School of Medicine (approval number, 2022-057). Blood tissue of young and old human was collected with the approval of the Ethics Committee of Tongren Hospital Affiliated to Shanghai Jiao Tong University School of Medicine (approval number, 2022-046-01).

Declaration of competing interest

The authors declare that they have no known competing financial interests or personal relationships that could have appeared to influence the work reported in this paper.

Acknowledgments

This work was supported by the National Natural Science Foundation of China [grant number, 82272165 to W. Xu, 22207050 to L. Li], the Fundamental Research Funds for the Central Universities [grant number, YG2023ZD28 to W. Xu], Shanghai Jiao Tong University School of Medicine Research-Oriented Physician Program in Clinical Medicine [JYYJXYS20240822 to W. Xu], Changning District Health Committee Excellent Innovation Talent Training Project [grant number, RCJD2022S01 to W. Xu], Shanghai Jiao Tong University K.C. Wong Medical Fellowship Fund [to W. Xu].

Appendix A. Supplementary data

Supplementary data to this article can be found online at https://doi.org/10.1016/j.bioactmat.2025.03.012.

References

[1] Z. Liu, H.L. Lee, J.S. Suh, et al., The ERα/KDM6B regulatory axis modulates osteogenic differentiation in human mesenchymal stem cells, Bone Res. 10 (1) (2022) 3.
[2] T.D. Rachner, S. Khosla, L.C. Hofbauer, Osteoporosis: now and the future, Lancet 377 (9773) (2011) 1276–1287.
[3] Y. Peng, S. Wu, Y. Li, et al., Type H blood vessels in bone modeling and remodeling, Theranostics 10 (1) (2020) 426–436.
[4] J.H. Hwang, Y.S. Park, H.S. Kim, et al., Yam-derived exosome-like nanovesicles stimulate osteoblast formation and prevent osteoporosis in mice, J. Contr. Release 355 (2023) 184–198.

[5] A.M. Silva, S.R. Moura, J.H. Teixeira, et al., Long noncoding RNAs: a missing link in osteoporosis, Bone Res. 7 (2019) 10.
[6] C. Zhang, W. Zhang, D. Zhu, et al., Nanoparticles functionalized with stem cell secretome and CXCR4-overexpressing endothelial membrane for targeted osteoporosis therapy, J. Nanobiotechnol. 20 (1) (2022) 35.
[7] G. Huang, Q. Zhao, W. Li, et al., Exosomes: a new option for osteoporosis treatment, Medicine 101 (52) (2022) e32402.
[8] J. Li, P. Habibovic, H. Yuan, et al., Biological performance in goats of a porous titanium alloy-biphasic calcium phosphate composite, Biomaterials 28 (29) (2007) 4209–4218.
[9] V. Sharma, C.D. Mukhopadhyay, Exosome as drug delivery system: current advancements, Extracell Vesicle. 3 (2024) 100032.
[10] E. Tzng, N. Bayardo, P.C. Yang, Current challenges surrounding exosome treatments, Extracell Vesicle 2 (2023) 100023.
[11] R. Kalluri, V.S. LeBleu, The biology, function, and biomedical applications of exosomes, Science 367 (6478) (2020).
[12] K. Popowski, H. Lutz, S. Hu, et al., Exosome therapeutics for lung regenerative medicine, J. Extracell. Vesicles 9 (1) (2020) 1785161.
[13] K. Cheng, K. Malliaras, D. Shen, et al., Intramyocardial injection of platelet gel promotes endogenous repair and augments cardiac function in rats with myocardial infarction, J. Am. Coll. Cardiol. 59 (3) (2012) 256–264.
[14] K. Cheng, R. Kalluri, Guidelines for clinical translation and commercialization of extracellular vesicles and exosomes based therapeutics, Extracell Vesicle 2 (2023) 100029.
[15] Y. He, Y. Chen, The potential of exosomes for osteoporosis treatment: a review, Drug Des. Dev. Ther. 18 (2024) 979–989.
[16] C. Sheng, X. Guo, Z. Wan, et al., Exosomes derived from human adipose-derived stem cells ameliorate osteoporosis through miR-335-3p/Aplnr axis, Nano Res. 15 (10) (2022) 9135–9148.
[17] K. Zhang, K. Cheng, Stem cell-derived exosome versus stem cell therapy, Nat Rev Bioeng (2023) 1–2.
[18] Y. Xie, A. Ibrahim, K. Cheng, et al., Importance of cell-cell contact in the therapeutic benefits of cardiosphere-derived cells, Stem Cell. 32 (9) (2014) 2397–2406.
[19] H. Song, X. Li, Z. Zhao, et al., Reversal of osteoporotic activity by endothelial cell-secreted bone targeting and biocompatible exosomes, Nano Lett. 19 (5) (2019) 3040–3048.
[20] Y. Hu, R. Xu, C.Y. Chen, et al., Extracellular vesicles from human umbilical cord blood ameliorate bone loss in senile osteoporotic mice, Metabolism 95 (2019) 93–101.
[21] J. Li, G. Wu, W. Li, et al., Plasma exosomes improve peripheral neuropathy via miR-20b-3p/Stat3 in type I diabetic rats, J. Nanobiotechnol. 21 (1) (2023) 447.
[22] G.S. Baht, D. Silkstone, L. Vi, et al., Exposure to a youthful circulaton rejuvenates bone repair through modulation of β-catenin, Nat. Commun. 6 (2015) 7131.
[23] W. Yang, N. Ding, R. Luo, et al., Exosomes from young healthy human plasma promote functional recovery from intracerebral hemorrhage via counteracting ferroptotic injury, Bioact. Mater. 27 (2023) 1–14.
[24] A. Sahu, Z.J. Clemens, S.N. Shinde, et al., Regulation of aged skeletal muscle regeneration by circulating extracellular vesicles, Nat Aging 1 (12) (2021) 1148–1161.
[25] A. Dey Bhowmik, T. Das, A. Chattopadhyay, Chronic exposure to environmentally relevant concentration of fluoride impairs osteoblast's collagen synthesis and matrix mineralization: involvement of epigenetic regulation in skeletal fluorosis, Environ. Res. 236 (Pt 2) (2023) 116845.
[26] M. Chen, Y. Sun, Y. Hou, et al., Constructions of ROS-responsive titanium-hydroxyapatite implant for mesenchymal stem cell recruitment in peri-implant space and bone formation in osteoporosis microenvironment, Bioact. Mater. 18 (2022) 56–71.
[27] E.J. Cotter, P.P. Doran, W.G. Powderly, Progenitor cell types in HIV-1 infection: bioactivity and emerging targets for treatment, Curr. HIV Res. 7 (5) (2009) 508–518.
[28] K. Cheng, D. Shen, J. Smith, et al., Transplantation of platelet gel spiked with cardiosphere-derived cells boosts structural and functional benefits relative to gel transplantation alone in rats with myocardial infarction, Biomaterials 33 (10) (2012) 2872–2879.
[29] Y. Zhao, P. He, J. Yao, et al., pH/NIR-responsive and self-healing coatings with bacteria killing, osteogenesis, and angiogenesis performances on magnesium alloy, Biomaterials 301 (2023) 122237.
[30] A. Carter, K. Popowski, K. Cheng, et al., Enhancement of bone regeneration through the converse piezoelectric effect, A novel approach for applying mechanical stimulation, Bioelectricity 3 (4) (2021) 255–271.
[31] H.S. Son, J. Lee, H.I. Lee, et al., Benzydamine inhibits osteoclast differentiation and bone resorption via down-regulation of interleukin-1 β expression, Acta Pharm. Sin. B 10 (3) (2020) 462–474.
[32] B. Wu, J. Shang, S. Lin, et al., A novel role for RILP in regulating osteoclastogenesis and bone resorption, Lab. Invest. 103 (5) (2023) 100067.
[33] K. Beider, V. Voevoda-Dimenshtein, A. Zoabi, et al., CXCL13 chemokine is a novel player in multiple myeloma osteolytic microenvironment, M2 macrophage polarization, and tumor progression, J. Hematol. Oncol. 15 (1) (2022) 144.
[34] B. Kundu, V. Brancato, J.M. Oliveira, et al., Silk fibroin promotes mineralization of gellan gum hydrogels, Int. J. Biol. Macromol. 153 (2020) 1328–1334.
[35] H. Kim, T. Kim, B.C. Jeong, et al., Tmem64 modulates calcium signaling during RANKL-mediated osteoclast differentiation, Cell Metab. 17 (2) (2013) 249–260.
[36] A.D. Ter Braake, A.E. Smit, C. Bos, et al., Magnesium prevents vascular calcification in Klotho deficiency, Kidney Int. 97 (3) (2020) 487–501.
[37] Q.C. Li, C. Li, W. Zhang, et al., Potential effects of exosomes and their MicroRNA carrier on osteoporosis, Curr. Pharm. Des. 28 (11) (2022) 899–909.
[38] Q. Gan, L. Chen, H.P. Bei, et al., Artificial cilia for soft and stable surface covalent immobilization of bone morphogenetic protein-2, Bioact. Mater. 24 (2023) 551–562.
[39] H. Hosseinkhani, M. Hosseinkhani, F. Tian, et al., Ectopic bone formation in collagen sponge self-assembled peptide-amphiphile nanofibers hybrid scaffold in a perfusion culture bioreactor, Biomaterials 27 (29) (2006) 5089–5098.
[40] J. Huang, J. Peng, G. Cao, et al., Hypoxia-induced MicroRNA-429 promotes differentiation of mc3t3-E1 osteoblastic cells by mediating ZFPM2 expression, Cell. Physiol. Biochem. 39 (3) (2016) 1177–1186.
[41] C. Chevalier, S. Kieser, M. Çolakoğlu, et al., Warmth prevents bone loss through the gut microbiota, Cell Metab. 32 (4) (2020) 575–590.e7.
[42] L. Dalle Carbonare, M. Zanatta, A. Gasparetto, et al., Safety and tolerability of zoledronic acid and other bisphosphonates in osteoporosis management, Drug Healthc. Patient Saf. 2 (2010) 121–137.
[43] J. Rebo, M. Mehdipour, R. Gathwala, et al., A single heterochronic blood exchange reveals rapid inhibition of multiple tissues by old blood, Nat. Commun. 7 (2016) 13363.
[44] O.H. Jeon, M. Mehdipour, T.-H. Gil, et al., Systemic induction of senescence in young mice after single heterochronic blood exchange, Nat. Metab. 4 (8) (2022) 995–1006.
[45] T.A. Allen, D. Asad, E. Amu, et al., Circulating tumor cells exit circulation while maintaining multicellularity, augmenting metastatic potential, J. Cell Sci. 132 (17) (2019).
[46] L. Hosseini, P. Shahabi, A. Fakhari, et al., Aging and age-related diseases with a focus on therapeutic potentials of young blood/plasma, Naunyn-Schmiedebergs Arch Pharmacol 397 (1) (2024) 1–13.
[47] B. Zhang, D.E. Lee, A. Trapp, et al., Multi-omic rejuvenation and life span extension on exposure to youthful circulation, Nat Aging 3 (8) (2023) 948–964.
[48] Y. Li, X. Wang, C. Pan, et al., Myoblast-derived exosomal Prrx2 attenuates osteoporosis via transcriptional regulation of lncRNA-MIR22HG to activate Hippo pathway, Mol Med 29 (1) (2023) 54.
[49] R.Z. Yang, W.N. Xu, H.L. Zheng, et al., Exosomes derived from vascular endothelial cells antagonize glucocorticoid-induced osteoporosis by inhibiting ferritinophagy with resultant limited ferroptosis of osteoblasts, J. Cell. Physiol. 236 (9) (2021) 6691–6705.
[50] L. Hao, S. Huang, T. Huang, et al., Bone targeting miR-26a loaded exosome-mimetics for bone regeneration therapy by activating Wnt signaling pathway, Chem. Eng. J. 471 (2023) 144594.
[51] J. Cores, T.G. Caranasos, K. Cheng, Magnetically targeted stem cell delivery for regenerative medicine, J. Funct. Biomater. 6 (3) (2015) 526–546.
[52] K. Cheng, W.S. Kisaalita, Exploring cellular adhesion and differentiation in a micro-/nano-hybrid polymer scaffold, Biotechnol. Prog. 26 (3) (2010) 838–846.
[53] L. Yu, M. Hu, X. Cui, et al., M1 macrophage-derived exosomes aggravate bone loss in postmenopausal osteoporosis via a microRNA-98/DUSP1/JNK axis, Cell Biol. Int. 45 (12) (2021) 2452–2463.
[54] L.-M. Lei, F.-X.-Z. Li, X. Lin, et al., Cold exposure-induced plasma exosomes impair bone mass by inhibiting autophagy, J. Nanobiotechnol. 22 (1) (2024) 361.
[55] R. Shah, T. Patel, J.E. Freedman, Circulating extracellular vesicles in human disease, N. Engl. J. Med. 379 (10) (2018) 958–966.
[56] K.S. Lee, S.H. Yeom, M.K. Kim, et al., Therapeutic potential of human stem cell-derived extracellular vesicles in idiopathic pulmonary fibrosis, Extracell Vesicle 4 (2024) 100045.
[57] Z. Ding, Z.F. Greenberg, M.F. Serafim, et al., Understanding molecular characteristics of extracellular vesicles derived from different types of mesenchymal stem cells for therapeutic translation, Extracell Vesicle. 3 (2024) 100034.
[58] K.D. Popowski, P.C. Dinh, A. George, et al., Exosome therapeutics for COVID-19 and respiratory viruses, View 2 (3) (2021) 20200186.
[59] D. Zhu, S. Liu, K. Huang, et al., Intrapericardial exosome therapy dampens cardiac injury via activating Foxo3, Circ. Res. 131 (10) (2022) e135–e150.
[60] W.F. Lai, M. Lin, W.T. Wong, Tackling aging by using miRNA as a target and a tool, Trends Mol. Med. 25 (8) (2019) 673–684.
[61] L.J. Kubiatowicz, A. Mohapatra, N. Krishnan, et al., mRNA nanomedicine: design and recent applications, Explorations 2 (6) (2022) 20210217.
[62] Z. Huang, S. Liu, N. Lu, et al., Nucleus-specific RNAi nanoplatform for targeted regulation of nuclear lncRNA function and effective cancer therapy, Explorations 2 (5) (2022) 20220013.
[63] D. Shen, K. Cheng, E. Marbán, Dose-dependent functional benefit of human cardiosphere transplantation in mice with acute myocardial infarction, J. Cell Mol. Med. 16 (9) (2012) 2112–2116.
[64] D.K. Kim, G. Bandara, Y.E. Cho, et al., Mastocytosis-derived extracellular vesicles deliver miR-23a and miR-30a into pre-osteoblasts and prevent osteoblastogenesis and bone formation, Nat. Commun. 12 (1) (2021) 2527.
[65] M. Tu, J. Tang, H. He, et al., MiR-142-5p promotes bone repair by maintaining osteoblast activity, J. Bone Miner. Metabol. 35 (3) (2017) 255–264.
[66] R. Zhao, Y. Zhu, B. Sun, Exploration of the effect of mmu-miR-142-5p on osteoblast and the mechanism, Cell Biochem. Biophys. 71 (1) (2015) 255–260.
[67] F. Wang, H. Wei, C. Hu, et al., Experimental study on construction of tissue engineered bone by autologous oxygen release nano-bionic scaffold combined with bone morphogenetic protein-2 induced bone marrow mesenchymal stem cells, Journal of Biomaterials and Tissue Engineering 9 (2019) 1254–1260.
[68] G. Lv, Y. Chen, Z. Cheng, et al., Circ_0006873 sponges miR-142-5p to inhibit osteoblastic differentiation of hBMSCs via regulating PTEN/Akt signaling pathway, Ann. Clin. Lab. Sci. 52 (1) (2022) 48–59.

[69] Y. Du, H. Zhong, C. Yu, et al., Mir-142-5p inhibits the osteogenic differentiation of bone marrow mesenchymal stem cells by targeting Lhx8, Heliyon 9 (9) (2023) e19878.
[70] Z. Lou, Z. Peng, B. Wang, et al., miR-142-5p promotes the osteoclast differentiation of bone marrow-derived macrophages via PTEN/PI3K/AKT/FoxO1 pathway, J. Bone Miner. Metabol. 37 (5) (2019) 815–824.
[71] H. Liu, X. Zhang, M. Zhang, et al., Mesenchymal stem cell derived exosomes repair uterine injury by targeting transforming growth factor-β signaling, ACS Nano 18 (4) (2024) 3509–3519.
[72] N. Wang, X. Liu, Z. Tang, et al., Increased BMSC exosomal miR-140-3p alleviates bone degradation and promotes bone restoration by targeting Plxnb1 in diabetic rats, J. Nanobiotechnol. 20 (1) (2022) 97.
[73] F. Meng, G. Wang, F. Zhou, et al., Exosomes from young plasma alleviate osteoporosis through miR-217-5p-regulated osteogenesis of bone marrow mesenchymal stem cell, Compos. B Eng. 276 (2024) 111358.
[74] T. Xu, Y. Luo, J. Wang, et al., Exosomal miRNA-128-3p from mesenchymal stem cells of aged rats regulates osteogenesis and bone fracture healing by targeting Smad5, J. Nanobiotechnol. 18 (1) (2020) 47.
[75] M. Zhai, Y. Zhu, M. Yang, et al., Human mesenchymal stem cell derived exosomes enhance cell-free bone regeneration by altering their miRNAs profiles, Adv. Sci. 7 (19) (2020) 2001334.
[76] R.A. Haraszti, M.C. Didiot, E. Sapp, et al., High-resolution proteomic and lipidomic analysis of exosomes and microvesicles from different cell sources, J. Extracell. Vesicles 5 (2016) 32570.